

## Microscopic calculation of double-dipole excitations

B. A. Brown and V. Zelevinsky

*Department of Physics and Astronomy, and National Superconducting Cyclotron Laboratory,  
Michigan State University, East Lansing, Michigan 48824-1321*

N. Auerbach

*Raymond and Berverly Sackler Faculty of Sciences, School of Physics and Astronomy, Tel Aviv University,  
Ramat Aviv, Tel Aviv 69978, Israel*

(Received 11 May 2000; published 14 September 2000)

The double-dipole mode of excitation is calculated for  $^{16}\text{O}$  and  $^{40}\text{Ca}$  in a large shell-model basis space that includes a full  $2\hbar\omega$  basis. The energies, distribution of strength and the spin, isospin splittings are computed. Sum rules are obtained and compared to the shell model results.

PACS number(s): 21.60.Cs, 21.10.Dr, 21.10.Hw

### I. INTRODUCTION

In the last decade experimental and theoretical research has led to the discovery of double giant resonances—a giant resonance built on top of another giant resonance. The double-dipole resonance was first identified in a pion charge exchange reaction [1] and was predicted earlier [2]. Later the double dipole was detected in Coulomb excitation in heavy-ion reactions [3–5]. Properties of double dipole modes and other types of double resonances were studied and are reviewed in several review articles [2–4,6]. Theoretical studies have been mostly of the “macroscopic” type, introducing collective coordinates in the description of double giant resonances [2–4,6]. Some papers used semimicroscopic models in which the random phase approximation (RPA) was employed to define the collective phonon states. Some extensions of the RPA have also been suggested [7,8]. Truly microscopic calculations are very difficult. A shell-model calculation requires very large spaces involving configurations made up of particles excited to several major shells. One must therefore truncate the space and limit the calculation to one-particle–one-hole ( $1p-1h$ ) and two-particle–two-hole ( $2p-2h$ ) configurations involving particles and holes in several major shells. Studies of this type were performed for some nuclei a few years ago [9].

In this work we present shell-model calculations of the double giant dipole state in  $^{16}\text{O}$  and  $^{40}\text{Ca}$ . By choosing light nuclei we are able to include a relatively large space of  $1p-1h$  and  $2p-2h$  configurations and therefore are able to study in detail the distribution of strength and the splitting of strength into the various allowed spin and isospin components. In the case of  $^{16}\text{O}$  we are able to account for the coupling of  $J^\pi=0^+$  and  $2^+$ ,  $1p-1h$  states to the corresponding  $2p-2h$  configurations. We also discuss energy weighted sum rules (EWSR) and the relationship between these sum rules for the single and double giant resonances (see also Ref. [10]). The sum rules are evaluated in the shell model basis (numerically) and in a boson model.

### II. SUM RULES

For the transition from an initial eigenstate  $|J_i, i\rangle$  to a set of final eigenstates  $|J_f, f\rangle$ , the energy weighted sum rule for

the dipole operator  $D$  is defined in terms of reduced matrix elements by

$$\sum_{J_f, f} (E_{J_f, f} - E_{J_i, i}) \frac{|(J_f, f || D || J_i, i)|^2}{(2J_i + 1)} = S_1^{(1)}. \quad (1)$$

The dipole operator is given by a summation over the nucleons

$$D = \sum_a e_a r_a Y^{(1)}(\hat{r}_a). \quad (2)$$

The notation for  $S_m^{(k)}$  is for the nonenergy-weighted ( $k=0$ ) and energy-weighted ( $k=1$ ) sums of the single ( $m=1$ ) and double-dipole ( $m=2$ ) excitations. The summation over intermediate states can be expressed as an expectation value in the initial state of the double commutator of the dipole operator with the Hamiltonian, and when the velocity dependence and exchange terms of the potential and residual interaction are ignored one obtains the well-known Thomas-Reiche-Kuhn (TRK) sum rule value

$$S_1^{(1)}(\text{TRK}) = \frac{9}{4\pi} \sum_a \frac{\hbar^2 e_a^2}{2m_a}. \quad (3)$$

The numerical value of  $S_1^{(1)}(\text{TRK})$  for the dipole operator with the standard effective charges for protons and neutrons is  $14.82 NZ/A e^2 \text{ fm}^2 \text{ MeV}$ . It is usual to represent the change in the TRK sum rule due to the velocity dependent and exchange terms in the Hamiltonian with the aid of an enhancement factor  $\kappa$ :

$$S_1^{(1)} = S_1^{(1)}(\text{TRK})(1 + \kappa). \quad (4)$$

With the universal factor  $\kappa$ , the sum rule  $S_1^{(1)}$  is still independent of the initial state. Assuming that the dipole transition from the ground state  $J=0$  is saturated by a single giant resonance (GR) state  $J_n=1$  at excitation energy  $E_1$ , we get

$$E_1 |(1 || D | 0)|^2 = 3S_1^{(1)}. \quad (5)$$

From the GR state  $|1\rangle$  there are transitions up to the two phonon states  $|2;J\rangle$ ,  $J=0,2$ , with transition energies  $E_{2;J} - E_1$  and the deexcitation transition to the ground state  $|0\rangle$  with transition energy  $-E_1$ . The sum rule (1) for the initial state  $|1\rangle$  reads

$$S_1^{(1)} = \frac{1}{9} \left\{ \sum_{2;J} (E_{2;J} - E_1) |(2;J||D||1)|^2 - E_1 |(0||D||1)|^2 \right\} \quad (6)$$

or, using Eq. (5) again,

$$\sum_{2;J} (E_{2;J} - E_1) |(2;J||D||1)|^2 = 12S_1^{(1)}. \quad (7)$$

Eliminating  $S_1^{(1)}$ , we obtain a relation between the observables (transition strengths and transition energies)

$$\sum_{2;J} (E_{2;J} - E_1) |(2;J||D||1)|^2 = 4E_1 |(1||D||0)|^2. \quad (8)$$

For the double-dipole excitation we are able (after simple algebra) to derive a relationship for the ratio of the excitation to the  $J=2$  and  $J=0$  (double-dipole) states

$$\frac{S_2^{(1)}(J=2)}{S_2^{(1)}(J=0)} = 5. \quad (9)$$

$S_2^{(1)}(J)$  is the energy weighted sum rule to the double-dipole state for a given final spin  $J$  defined by

$$S_2^{(1)}(J) = \sum_2 (E_{2;J} - E_0) \frac{|\sum_1 (2;J||D||1)(1||D||0)|^2}{3}, \quad (10)$$

where the sum  $\Sigma_2$  is over all two phonon states with a given  $J$ , and the  $\Sigma_1$  is over all single phonon states.

The above equations are in terms of the reduced matrix elements. We now express some of the results in terms of reduced transition probabilities which (with our definition of the reduced matrix elements) are given by

$$B(T_\lambda; i \rightarrow f) = \frac{1}{2J_i + 1} |(f||T_\lambda||i)|^2. \quad (11)$$

Our results expressed in terms of reduced transition probabilities are

$$|(1||D||0)|^2 = B(0 \rightarrow 1) = 3B(1 \rightarrow 0), \quad (12)$$

$$|(2;J||D||1)|^2 = 3B(1 \rightarrow 2;J) = (2J+1)B(2;J \rightarrow 1). \quad (13)$$

Equation (8) can now be written in two equivalent forms (excitation or deexcitation)

$$\sum_{2;J} (E_{2;J} - E_1) B(1 \rightarrow 2;J) = \frac{4}{3} E_1 B(0 \rightarrow 1), \quad (14)$$

$$\sum_{2;J} (E_{2;J} - E_1) (2J+1) B(2;J \rightarrow 1) = 12E_1 B(1 \rightarrow 0). \quad (15)$$

In the harmonic phonon limit when

$$E_1 = \omega, \quad E_{2;J} = 2\omega \quad (J=0,2), \quad (16)$$

we obtain

$$\frac{\sum_{2;J} B(1 \rightarrow 2;J)}{B(0 \rightarrow 1)} = \frac{4}{3}, \quad \frac{B(2;J \rightarrow 1)}{B(1 \rightarrow 0)} = 2. \quad (17)$$

For independent bosons of multipolarity  $l$ , the normalized one-boson and two-boson states are

$$|1;lm\rangle = b_{lm}^\dagger |0\rangle \quad (18)$$

and

$$|2;JM\rangle = \frac{1}{\sqrt{2}} \sum_{mm'} C_{lm\,lm'}^{JM} b_{lm}^\dagger b_{lm'}^\dagger |0\rangle, \quad (19)$$

$$J=0,2,\dots,2l \text{ (even)}.$$

If the transition operator is proportional to the boson coordinate  $T_{lm} \propto (b_{lm}^\dagger + b_{l\bar{m}})$ , the ratio of reduced deexcitation probabilities for all two-boson states is the same and given by the Bose factor

$$\frac{B(2;J \rightarrow 1)}{B(1 \rightarrow 0)} = 2. \quad (20)$$

For excitation transitions, the ratio

$$R_J = \frac{B(1 \rightarrow 2;J)}{B(0 \rightarrow 1)} = \frac{2}{(2l+1)^2} (2J+1) \quad (21)$$

is proportional to the statistical weight  $(2J+1)$  of the two-boson state  $|JM\rangle$ . For the total reduced probability of all two-boson states, we obtain

$$\sum_J R_J = \frac{2}{(2l+1)^2} \sum_J (2J+1). \quad (22)$$

For the sum in Eq. (22), where  $J$  is even, one finds  $\sum_J (2J+1) = (2l+1)(l+1)$  and hence

$$\sum_J R_J = \frac{\sum_J B(1 \rightarrow 2;J)}{B(1 \rightarrow 0)} = \frac{2l+2}{2l+1}. \quad (23)$$

For dipole excitations where  $l=1$  this ratio is  $4/3$ . The general boson model results of Eqs. (20) and (23) agree with the specific results of Eq. (17) obtained above with the dipole sum-rule model.

Up to now we did not specify the isospin quantum numbers of the excitation. Since we will be working in a given  $N=Z$  nucleus and discussing the dipole excitation within the states of this nucleus, our excitation operator is an isovector

TABLE I. Transition strengths and average energies for the single states. The quantities are defined in the text.

$e^2 \text{ fm}^2$	$B(1 \rightarrow 0)$	$S_1^{(0)}$ $e^2 \text{ fm}^2$	$S_1^{(1)}$ $e^2 \text{ fm}^2 \text{ MeV}$	$\bar{E}_1$ $\text{MeV}$
$^{16}\text{O } 0s-0p-1s0d-1p0f$	1.49	4.48	106	25
$^{16}\text{O } 0p-1s0d$	1.49	4.48	106	25
$^{40}\text{Ca } 1s0d-1p0f$	4.60	13.80	268	20

$\Delta T=1$ , with projection  $\Delta T_3=0$ . Then the double-dipole states with  $J=0$  or 2 can have  $T=0$  or 2 and  $T_3=0$ , and in the simple boson model, the intensities of the branches with  $T=0$  or 2 are predicted to differ by the squared Clebsch-Gordan coefficient  $[C_{10\ 10}^{\Delta T 0}]^2$ . Therefore the intensity of the branch  $T=2$  should exceed that for  $T=0$  by a factor of 2. The isospin dependence of the strength for nuclei with a neutron excess has been discussed in Ref. [15].

### III. NOTATION FOR SHELL-MODEL DIPOLE MATRIX ELEMENTS

The microscopic results presented in the next section are discussed in terms of the following notation which is specific for dipole transitions. We use the  $\langle \rangle$  matrix element notation to distinguish these microscopic results from the sum-rule and boson model results expressed in terms of  $()$  matrix elements. We also introduce an explicit index  $f$  for the final states. The dipole matrix element from the  $0^+$  ground state to a specific single-dipole final state  $|1^-, f\rangle$  is given by

$$S_{1,f}^{(0)} = |\langle 1^-, f || D || 0^+ \rangle|^2, \quad (24)$$

TABLE II. Transition strengths and average energies for the double-dipole states. The quantities are defined in the text.

Nucleus model space	$J$	$T$	$B(2 \rightarrow 1)$ $e^2 \text{ fm}^2$	$S_2^{(0)}$ $e^4 \text{ fm}^4$	$S_2^{(1)}$ $e^4 \text{ fm}^4 \text{ MeV}$	$\bar{E}_2$ $\text{MeV}$
$^{16}\text{O}$ $0s-0p-1s0d-1p0f$	0+2	0+2	5.30	26.4	1176	44.6
	1	0	0.33	0	0	
	0	0+2	2.65	4.4	189	43.7
	2	0+2	2.65	21.9	984	44.9
	0+2	0	2.43	12.1	492	40.7
	0+2	2	2.88	14.3	684	48.0
$^{16}\text{O}$ $0p-1s0d$	0+2	0+2	4.68	23.6	1048	44.4
	1	0	0.28	0	0	
	0	0+2	2.37	3.9	171	43.6
	2	0+2	2.31	19.7	876	44.5
	0+2	0	1.80	9.1	354	39.0
	0+2	2	2.88	14.5	694	47.8
$^{40}\text{Ca}$ $1s0d-1p0f$	0+2	0+2	16.3	233	9200	39.3
	1	0	0.36	0	0	
	0	0+2	8.2	39	1522	39.1
	2	0+2	8.1	195	7677	39.4
	0+2	0	5.9	85	3135	36.9
	0+2	2	10.4	148	6064	40.8

and the energy-weighted matrix element to a specific final state is

$$S_{1,f}^{(1)} = E_{1,f} |\langle 1^-, f || D || 0^+ \rangle|^2. \quad (25)$$

We define the ground state energy as  $E_{\text{g.s.}}=0$ .

The double-dipole strength to a specific final state  $f$  is given by

$$S_{2,f}^{(0)}(J,T) = \sum_n \frac{|\langle J,T,f || D || 1_n^- \rangle \langle 1_n^- || D || 0^+ \rangle|^2}{3}. \quad (26)$$

The spin of the final state can be  $0^+$ ,  $1^+$ , or  $2^+$ . The corresponding energy-weighted double-dipole strength to a given final state is

$$S_{2,f}^{(1)}(J,T) = E_{2,f} \sum_n \frac{|\langle J,T,f || D || 1_n^- \rangle \langle 1_n^- || D || 0^+ \rangle|^2}{3}. \quad (27)$$

The strength summed over all final states for the single ( $m=1$ ) and double-dipole ( $m=2$ ) states is given by

$$S_m^{(k)} = \sum_f S_{m,f}^{(k)}. \quad (28)$$

We define the average energy of the single and double dipole state as

$$\bar{E}_m = S_m^{(1)} / S_m^{(0)}. \quad (29)$$

Finally we introduce the reduced transition probabilities

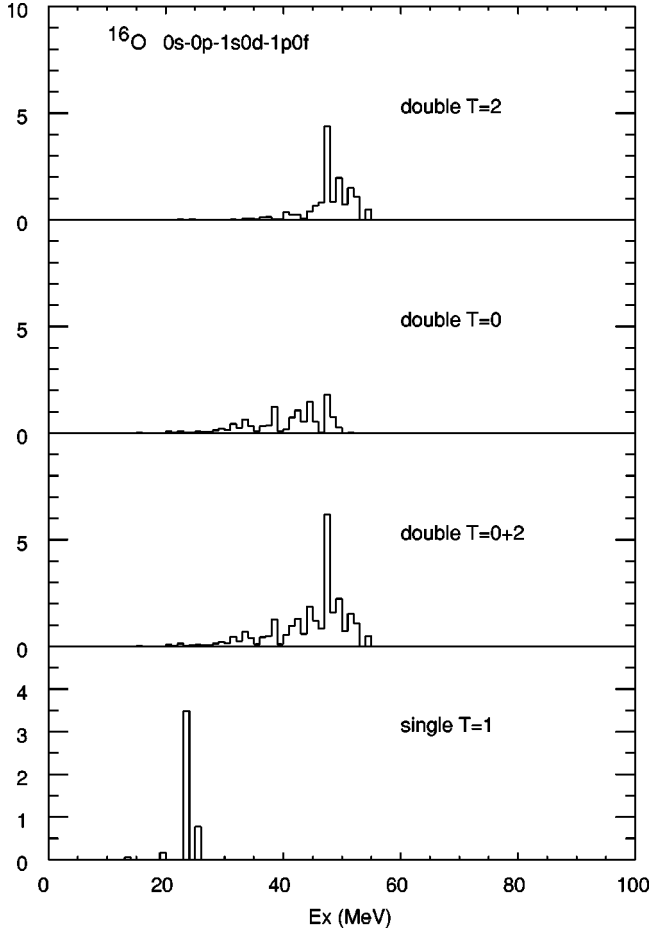


FIG. 1. Single and double-dipole strength distributions in the  $0s-0p-1s0d-1p0f$  model space for  $^{16}\text{O}$ . The double-dipole strength is summed over  $J=0^+$  and  $2^+$  and is shown as a function of various isospins of the double excitation. The units are  $e^2 \text{ fm}^2/\text{MeV}$  for single-dipole excitation and  $e^4 \text{ fm}^4/\text{MeV}$  for the double-dipole excitation.

$$B(1 \rightarrow 0) = \sum_f \frac{|\langle 1^-, f || D || 0^+ \rangle|^2}{3} = \frac{S_1^{(0)}}{3} \quad (30)$$

and

$$B(2; J, T \rightarrow 1) = \sum_f \frac{|\langle J, T, f || D || 1_n^- \rangle|^2}{(2J+1)}, \quad (31)$$

where  $n$  is taken to be the  $1^-$  which has the strongest single-dipole excitation from the ground state. In our examples the isospin quantum numbers are  $T=0$  and  $T_z=0$  for the ground state,  $T=1$  and  $T_z=0$  for the single-dipole states and  $T=0, 1, 2$  and  $T_z=0$  for the double dipole states.

#### IV. SHELL-MODEL CALCULATIONS

The shell-model calculations are carried out in a basis where  $|0^+\rangle$  is the closed-shell  $0\hbar\omega$  configuration,  $|1_n^-\rangle$  are the  $1p-1h$   $1\hbar\omega$  configurations, and  $|J_f^+\rangle$  are the  $1p-1h$  and  $2p-2h$   $2\hbar\omega$  configurations. This is equivalent to a Tamm-Dancoff (TDA) truncation of the dipole excitation from the

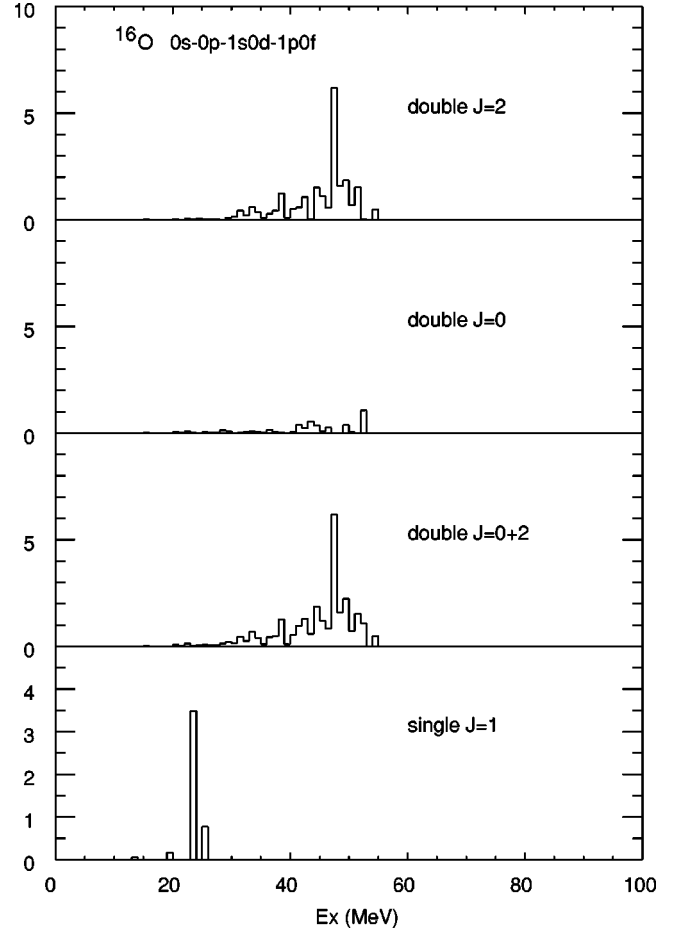


FIG. 2. Single and double-dipole strength distributions in the  $0s-0p-1s0d-1p0f$  model space for  $^{16}\text{O}$ . The double-dipole strength is summed over  $T=0$  and  $2$  and is shown as a function of various spins of the double excitation. The units are  $e^2 \text{ fm}^2/\text{MeV}$  for single-dipole excitation and  $e^4 \text{ fm}^4/\text{MeV}$  for the double-dipole excitation.

ground state and the dipole excitation from the single-dipole state.

For  $^{16}\text{O}$  one set of calculations was carried out in a model space which included the  $0s$ ,  $0p$ ,  $1s0d$ , and  $1p0f$  shells. The Hamiltonian is the WBP interaction from Ref. [11] which was determined by a least-squares fit of the particle-hole two-body matrix elements to the binding energies and excitation energies of nuclei in the  $A=10-20$  mass region. There are five  $1\hbar\omega$   $1^-$   $T=1$  states, 630  $2p-2h$   $2\hbar\omega$  states, and 36  $1p-1h$   $2\hbar\omega$  states (with  $J^\pi=0^+$ ,  $1^+$ , and  $2^+$  and with  $T=0, 1$ , and  $2$ ). For  $A=16$  we use harmonic-oscillator radial wave functions with  $\hbar\omega=13.92$  MeV for the dipole matrix elements. The double-dipole strength arises from (A) two ‘‘parallel’’  $0p \rightarrow 1s0d$  transitions from the closed shell leading to the  $2p-2h$   $2\hbar\omega$  states, or (B) from a  $0p \rightarrow 1s0d$  transition from the closed shell followed by a  $0s \rightarrow 0p$  or a  $1s0d \rightarrow 1p0f$  transition to the  $1p-1h$   $2\hbar\omega$  states.

We also carry out the calculation in a reduced model space which includes only the  $0p$  and  $1s0d$  shells. In this model space the  $2\hbar\omega$  basis does not include the 36  $1p-1h$   $2\hbar\omega$  states (excitation path B). Comparison of the results in

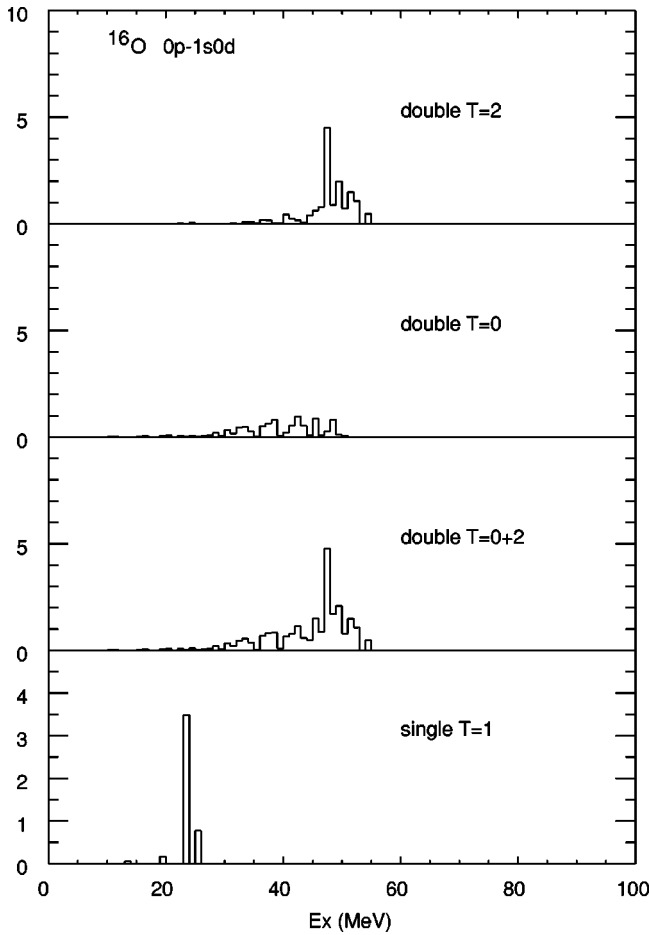


FIG. 3. Single and double-dipole strength distributions in the  $0p-1s0d$  model space for  $^{16}\text{O}$ . The double-dipole strength is summed over  $J=0^+$  and  $2^+$  and is shown as a function of various isospins of the double excitation. The units are  $e^2 \text{ fm}^2/\text{MeV}$  for single-dipole excitation and  $e^4 \text{ fm}^4/\text{MeV}$  for the double-dipole excitation.

the  $0p-1s0d$  and  $0s-0p-1s0d-1p0f$  model spaces will show the importance of including the  $1p-1h$   $2\hbar\omega$  states which incorporate the giant monopole and quadrupole resonances.

The results for  $^{40}\text{Ca}$  were obtained in the  $1s0d-1p0f$  model space using the WBMB interaction from Ref. [12]. In this model space there are eight  $1^-$ ,  $T=1$   $1\hbar\omega$  states and 3386  $2p-2h$   $2\hbar\omega$  states. The harmonic-oscillator parameter for  $A=40$  is  $\hbar\omega=11.02$  MeV. For  $^{40}\text{Ca}$  a model space which incorporates the  $1p-1h$   $2\hbar\omega$  states is not available. In the above model spaces the Hamiltonian was diagonalized and the quantities defined in the previous section were evaluated.

## V. RESULTS AND DISCUSSION

In Tables I and II we present the values of the basic quantities defined in Sec. IV. In Figs. 1–5 the distributions of  $S_{m,f}^{(0)}$  vs excitation energy are shown. In Figs. 1, 3, and 4, the comparisons are made in terms of specific final isospins  $T$  of the double dipole (summed over  $J$ ). In Figs. 2 and 5 the

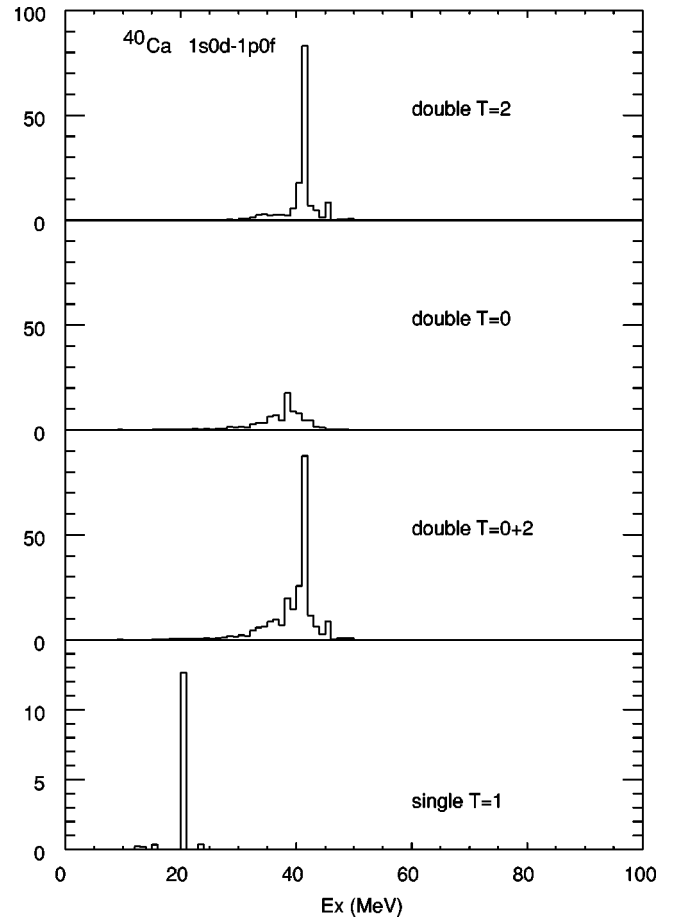


FIG. 4. Single- and double-dipole strength distributions in the  $1s0d-1p0f$  model space for  $^{40}\text{Ca}$ . The double-dipole strength is summed over  $J=0^+$  and  $2^+$  and is shown as a function of various isospins of the double excitation. The units are  $e^2 \text{ fm}^2/\text{MeV}$  for single-dipole excitation and  $e^4 \text{ fm}^4/\text{MeV}$  for the double-dipole excitation.

comparisons are made in terms of specific final spins  $J$  (summed over  $T$ ).

The energy weighted sum  $S_1^{(1)}$  for the single-dipole strength (Table I) is about a factor of 2 larger than the TRK sum rule values of  $59 e^2 \text{ fm}^2 \text{ MeV}$  for  $^{16}\text{O}$  and  $148 e^2 \text{ fm}^2 \text{ MeV}$  for  $^{40}\text{Ca}$ . However, it is well known that the results of the TDA (used also in Ref. [8]) and the RPA differ significantly for the states with a high degree of collectivity. The TDA truncation which we employ does not conserve the TRK sum rule. One must use the RPA or a larger shell-model space which includes ground state (RPA-type) correlations. For the single-dipole excitation we can include  $2p-2h$  configurations in the ground state and  $3p-3h$  configurations in the  $1^-$  states. In  $^{16}\text{O}$  this brings the energy weighted sum rule down to about  $82 e^2 \text{ fm}^2 \text{ MeV}$ . The enhancement factor is thus about  $\kappa=0.4$  which is typical of those found with realistic interactions (see page 714 in Ref. [13]). Although we cannot carry out the equivalent ‘‘RPA’’ extension of the shell model for the double-dipole states, we expect that there will be an equivalent TDA to RPA reduction in the double-dipole sum rules. The other caveat in our comparison between experiment and theory is that our cal-

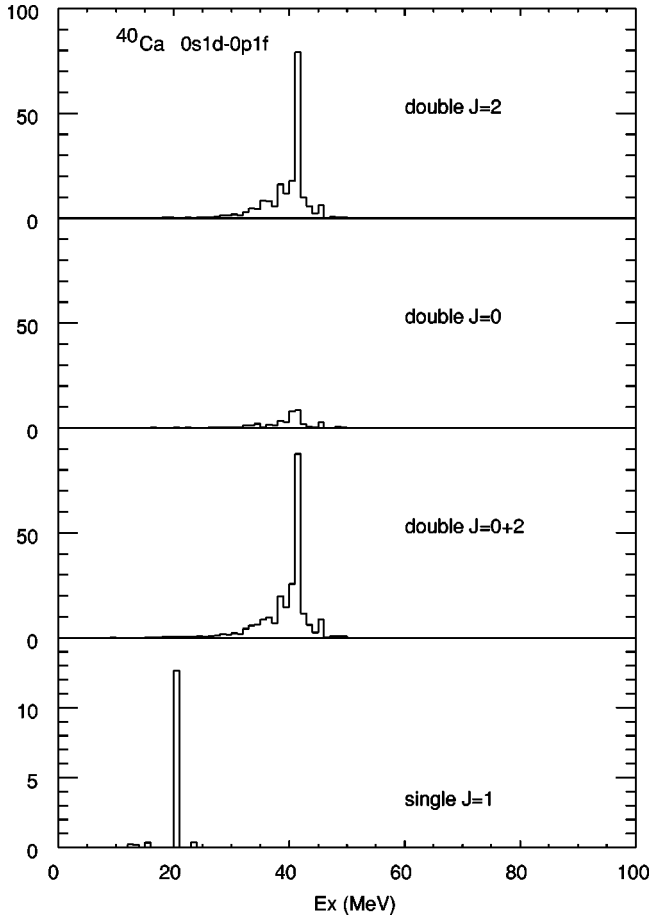


FIG. 5. Single and double-dipole strength distributions in the  $1s0d-1p0f$  model space for  $^{40}\text{Ca}$ . The double-dipole strength is summed over  $T=0$  and  $2$  and is shown as a function of various spins of the double excitation. The units are  $e^2 \text{fm}^2/\text{MeV}$  for single-dipole excitation and  $e^4 \text{fm}^4/\text{MeV}$  for the double-dipole excitation.

calculations do not include the spreading width or decay width. Thus our theoretical strength distributions must be folded with another distribution which will be  $J$  and  $T$  dependent. We will concentrate in this discussion on ratios of the strengths and how they depend on  $J$  and  $T$ .

In the boson model, one cannot have  $J=1^+$  for the double dipole. The total  $B(1 \rightarrow 2)$  strength we obtain to the  $1^+$  is much smaller than to  $0^+$  and  $2^+$  (see Table II), and the energy weighted double-dipole strength  $S_2^{(1)}$  to each  $1^+$  state turns out to be identically zero, as well as the  $B(1 \rightarrow 2)$  and double-dipole strength to all  $T=1$  states (see also the discussion in Ref. [8]).

We first discuss the results of the  $0s-0p-1s0d-1p0f$  model space shown in Figs. 1 and 2. In the bottom part of Fig. 1 we show the distribution of the  $J=1^-$ ,  $T=1$  single-dipole strength. In the parts above it, is the double-dipole strength broken down into various final isospin values (and summed over all final spin values). We see that the total double-dipole strength distribution is broader than the single dipole but is still rather well concentrated. The double-dipole energy in  $^{16}\text{O}$  is lower than twice the energy of the single dipole. This departure from harmonicity can also be seen in

Tables I and II where the average energy  $\bar{E}_1$  is at 25 MeV while the  $\bar{E}_2$  is at 44.6 MeV, about 5 MeV below the harmonic limit of  $2\bar{E}_1$ . The upper two parts in Fig. 1 show the distribution of strength separately for the two isospin components. One can see that the  $T=2$  is stronger than  $T=0$  and that they are shifted by about 7 MeV (see Table II). The spreading is greater in the  $T=0$  state than in the  $T=2$  state. In addition the decay width of the  $T=0$  should be much larger than for  $T=2$ . This means that a concentration of double-dipole strength observed experimentally is likely to represent only the  $T=2$  fraction of the total distribution.

In Fig. 2 we show the results of the  $^{16}\text{O}$   $0s-0p-1s0d-1p0f$  calculation with the strength separated into the  $J=0^+$  and  $2^+$  components. The summed results in Table II can be compared with the sum-rule and boson models. The ratio of  $J=2$  to  $J=0$  energy-weighted strength is 5.2, very close to the value of 5 from Eq. (9). The expectation that the  $B(2 \rightarrow 1)$  value is independent of  $J$  from the boson model, Eq. (20), is exactly satisfied in the calculation. The calculated value of 1.78 for the ratio  $B(2 \rightarrow 1)$  to  $B(1 \rightarrow 0)$  is a little smaller than the value of two expected from Eqs. (17) and (20). Thus we do not find any significant deviations from the analytical results.

In Fig. 3 we show the results of the smaller  $0p-1s0d$  space calculation of  $^{16}\text{O}$ . In this case the double dipole does not contain the  $1p-1h$  configuration in which the particle is lifted two shells into a  $2\hbar\omega$  excitation to form  $J=0^+$  and  $2^+$   $T=0$  states which are admixed into the  $2p-2h$  configurations. The effect of these is to increase the double-dipole strength by about 15% but not having any substantial effect on location and width of the distribution.

The results for  $^{40}\text{Ca}$  are shown in Figs. 4 and 5. The single dipole distribution is characterized by a single strong peak at 20 MeV. The peak energy of the combined  $T=0$  and  $T=2$  strength of the double dipole is at 40 MeV, at twice the energy of the single-dipole. The same is true for the average energies in Table II. The harmonic limit of  $\bar{E}_2=2\bar{E}_1$  is obeyed much better than in  $^{16}\text{O}$ . It has been pointed out in Ref. [14] that anharmonicities decline quickly with increasing mass number. The comparison of the total strengths given in Table II to the analytical models is quite similar for the  $^{16}\text{O}$   $0p-1s0d$  and  $^{40}\text{Ca}$   $1s0d-1p0f$  calculations.

In Table II we also present the isospin decomposition of the double-dipole strength. We see from Table II that the  $0p-1s0d$  calculation for  $^{16}\text{O}$  and the  $1s0d-1p0f$  calculation for  $^{40}\text{Ca}$  give a ratio of about a factor of 2 for the  $T=2$  to  $T=0$  strength in agreement with that expected from the ratio of isospin Clebsch-Gordan coefficients discussed in Sec. II. For the complete  $0s-0p-1s0d-1p0f$  model-space calculation of  $^{16}\text{O}$  only the  $T=0$  transition strength is changed by the inclusion of the  $1p-1h$   $2\hbar\omega$  (B-type) states since they can only couple to  $T=0$  (or  $T=1$ ). The strength of this  $T=0$  component is increased by about 25% making the total strength more equal for the  $T=0$  and  $T=2$  channels.

#### ACKNOWLEDGMENT

This work was supported by the U.S.-Israel Binational Science Foundation and by NSF Grant No. PHY-9605207.

- [1] S. Mordechai *et al.*, Phys. Rev. Lett. **61**, 531 (1988).
- [2] N. Auerbach, *Proceedings of the Pion-Nucleus International Workshop* (AIP, New York, 1988), p. 34; N. Auerbach, Ann. Phys. (N.Y.) **197**, 376 (1990).
- [3] For a review see T. Aumann, P. F. Bortignon, and H. Emling, Annu. Rev. Nucl. Part. Sci. **48**, 351 (1998); A. Bertulani and V. Yu. Ponomarev, Phys. Rep. **321**, 139 (1999).
- [4] P. Chomaz and N. Frascaria, Phys. Rep. **252**, 275 (1995).
- [5] C. A. Bertulani and V. Zelevinsky, Phys. Rev. Lett. **71**, 967 (1993); Nucl. Phys. **A568**, 931 (1994).
- [6] C. A. Bertulani and G. Baur, Phys. Rep. **163**, 299 (1988).
- [7] F. Catara, P. Chomaz, and A. Vitturi, Nucl. Phys. **A471**, 661 (1987).
- [8] C. A. Bertulani, V. Yu. Ponomarev, and V. V. Voronov, Phys. Lett. B **388**, 374 (1996).
- [9] S. Nishizaki and J. Wambach, Phys. Rev. C **57**, 1515 (1998).
- [10] H. Kurasawa and T. Suzuki, Nucl. Phys. **A597**, 374 (1996).
- [11] E. K. Warburton and B. A. Brown, Phys. Rev. C **46**, 923 (1992).
- [12] E. K. Warburton, J. A. Becker, and B. A. Brown, Phys. Rev. C **41**, 1147 (1990).
- [13] *Theoretical Nuclear Physics Vol I: Nuclear Structure*, edited by A. deShalit and H. Feshbach (Wiley, New York, 1974).
- [14] G. F. Bertsch, P. F. Bortignon, and K. Hagino, Nucl. Phys. **A471**, 1 (1999).
- [15] A. F. R. de Toledo Piza, M. S. Hussein, B. V. Carlson, C. A. Bertulani, L. F. Canto, and S. Cruz-Barrios, Phys. Rev. C **59**, 3093 (1999).